Chaos, Solitons and Fractals 172 (2023) 113584

Contents lists available at ScienceDirect

Chaos, Solitons and Fractals

journal homepage: www.elsevier.com/locate/chaos

# Mathematical modeling of anomalous diffusive behavior in transdermal drug-delivery including time-delayed flux concept

Milena Čukić [a], Slobodanka Galovic [b,*]

[a] Empa, Swiss Federal Institute for Materials Science and Technology, Laboratory for Biomimetic Membranes and Textiles, Lerchenfeldstrasse 5, 9014 St. Gallen, Switzerland

[b] Vinca Institute of Nuclear Sciences-National Institute of the Republic of Serbia, University of Belgrade, Mike Petrovica Alasa 12-14, 522, 11001 Belgrade, Serbia

ARTICLE INFO

*Keywords:*
Anomalous diffusion
Fractional calculus
Time-delayed flux
Skin membrane
Drug delivery

ABSTRACT

Molecular transport through a composite multilayer membrane is a central process in transdermal drug delivery (TDD). Classical Fickean approach treats skin as a pseudo-homogenous membrane, while in reality skin is highly heterogeneous system as shown in basic physiological research. Particle transport across such systems shows anomalous diffusive behavior that is described by fractional models. These models don't consider experimentally observed dependence of particle transport nature on time scale. The possible way of inclusion of that observation in model of transdermal transport is presented in this paper. The generalized fractional models of the spectral functions of the concentration profile and the cumulative amount of the drug absorbed through the bloodstream are derived. The derived model predicts resonances in concentration profile and larger cumulative amount of the drug in both the short-time limit and the long-time limit, which can have significant physiological implications.

## 1. Introduction

Transdermal drug delivery is technology being increasingly used as a safe alternative to classical medication route. Transdermal patches are considered pharmaceutical devices that contain drug and can be applied to deliver molecules of active substance to circulation via unbroken skin. This transdermal penetration of various hydrophilic, lipophilic, or even hydrophobic drugs can be modeled as a mass diffusion through the skin membrane, for which the main obstacle (or barrier) in case of human skin is its upper most layer, the stratum corneum (SC). This layer is composed of flattened dead cells (corneocytes) embedded in a matrix of staked lipid lamellae comprises free fatty acids, ceramides and cholesterol (Fig. 1).

Many papers have addressed various aspects of transdermal drug delivery [1–4] where different models of skin permeability have been proposed [1,5–7]. The good review of the state-of-the-art of skin transport modeling can be find in [8,9]. In all of those models diffusion of molecules is modeled in terms of Fick's laws (Fick's first and second laws) or from statistical physics point of view as a Brownian process. These approaches completely neglect the possibility—or likelihood of—occurrence of anomalous diffusion caused by highly heterogeneous structure of skin.

Some of examples of anomalous diffusion are charge carrier motion in amorphous semiconductors [10,11], molecular motor-driven motion in biological cells [12,13], motion of particles in crowded environments such as biological membranes [14–16], chemical migration in porous media [17,18], etc. It is interesting to note that similar problems occur in the heat transport problems where classic diffusion theory of heat conduction cannot explain experimentally observed anomalous effects [19–21].

In many highly heterogeneous media, there is strong experimental evidence that deviations from the behavior predicted by classical diffusion theory have been observed [22–26]. Anomalous-diffusion emerges due to a variety of physical mechanism, e.g., trapping interaction or the viscoelasticity of the environment but it is always related to non-Brownian motion of mass and energy carriers [22–26].

Classical Brownian motion, or pedesis, the random motion of inert particles suspended in a simple liquid or gas, is characterized by the linear time dependence of the mean squared displacement $\langle x^2(t) \rangle = 2Dt$ with the diffusion constant D of physical dimension $m^2/s$ [27,28], as experimentally verified by Nordlund in 1914 [29]. Deviation from the linear time dependence of the MSD of Brownian motion are observed across many areas of science, techniques and technology [30–35] and frequently have the power-law dependence $\langle x^2(t) \rangle \simeq D_\gamma t^\gamma$, in terms of

* Corresponding author.
*E-mail address:* bobagal@vin.bg.ac.rs (S. Galovic).

https://doi.org/10.1016/j.chaos.2023.113584
Received 2 April 2023; Received in revised form 9 May 2023; Accepted 13 May 2023
Available online 30 May 2023

the anomalous diffusion exponent $\gamma$ and the generalized diffusion coefficient $D_\gamma$ of physical dimension length$^2$/time$^\gamma$ [22,23,26,36–38]. If $0 < \gamma < 1$ than there is subdiffusion. If $\gamma > 1$ than there is superdiffusion. The normal diffusion is characterized by$\gamma = 1$.

The best-known stochastic processes, which can explain anomalous diffusion behavior, include fractional Brownian motion (Levy model) and the continuous time random walk (CTRW). CTRWs with power-law waiting time (or transition time) can be mapped onto time-fractional diffusion equations [36–40]. In general, the magnitude of anomalous diffusive exponent $\gamma$ can be related by fractionality of the random walk of the particles across heterogeneous structure (non ergodicity of random walk, or in continuum approximation to memory properties of the media across with particles move) while the generalized diffusion coefficient $D_\gamma$ can be related with fractality of heterogeneous structure [23,26,38]. In particular, various aspects of transdermal delivery based on subdiffusive fractional generalization with local heat flux concept [41–45], show that the introduction of the fractional derivative offers a better description of the diffusion processes in the SC layer in comparison to other classical models.

Recently, researches have made and promoted remarkable progress towards improving experimental techniques for investigation of diffusive processes, mainly illustrated in single-particle tracking (SPT) technique [46–48]. Such improvement yield novel insight into transport properties of particles across biological system [46–52] and nanomaterials [53–55], where the high resolution of the experiments has found anomalous diffusive behaviors depending on the time scale, i.e. time non-locality of transport process. In order to capture that behavior, we have suggested in this paper an application of fractional generalization of classic diffusion including time-delayed flux.

The organization of this paper is as follows: after the introductory section, in Section 2 the fractional generalized transport equation that includes non-local heat flux in one-dimensional approximation is briefly presented and explained. In Section 3, a serious problem of drug transport through the skin is presented, based on the generalized approach presented in Section 2, and the application of the Laplace's transform. In Section 4, the spectral functions of the drug concentration and the cumulative amount of the drug were analyzed and discussed. Finally, the most important conclusions were made in the last section.

## 2. Generalized fractional diffusion theory including delayed flux

The classical theory of the particle transport or the Fick's second law describes particle transport as diffusion process by the following partial differential equation [56]:

$$\frac{\partial \rho(x,t)}{\partial t} = D\frac{\partial^2 \rho(x,t)}{\partial x^2} \tag{1}$$

The Eq.1 is a consequence of the continuity equation:

$$\frac{\partial \rho(x,t)}{\partial t} = -\frac{\partial j(x,t)}{\partial x} \tag{2}$$

and constitutive relation known as Fick's first law:

$$j(x,t) = -\mathrm{D}\frac{\partial \rho(x,t)}{\partial x} \tag{3}$$

In Eqs. 1–3 with symbols $j(\boldsymbol{x},t)$and $\rho(\boldsymbol{x},t)$ are denoted particle flux and the distribution function of the diffusing quantity, respectively, while the symbol $D$ denotes diffusion constant [m$^2$/s].

Mathematically, Eq.1 is the parabolic partial differential equation. It is known that the equations of the parabolic type lead to a physically incorrect conclusion about the infinite speed of propagation of disturbances - the change in concentration at a given point in space is instantaneously manifested at infinitely distant point [37,57–61]. This is the consequence of the constitutive relation of the form given by Eq.3

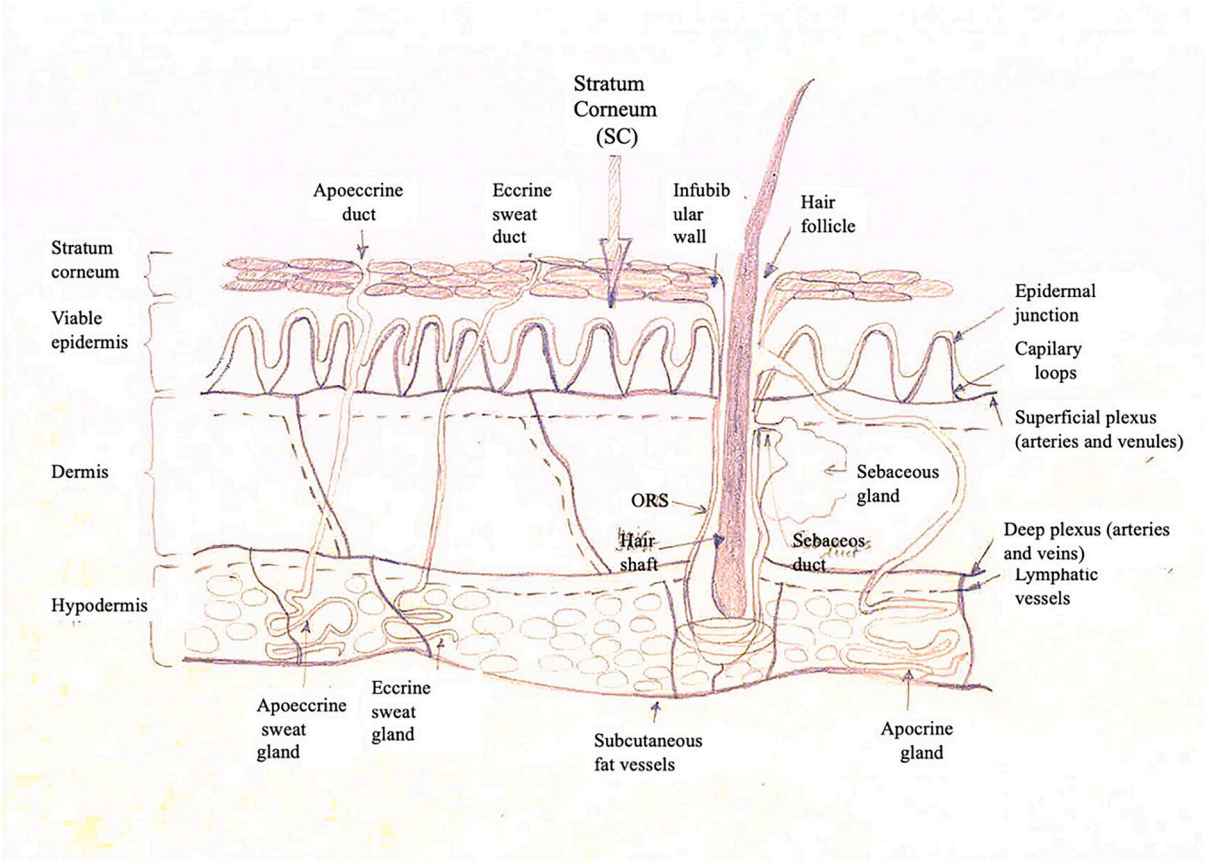


**Fig. 1.** Illustration of anatomical structure of the human skin.

that states that particle flux in the given point and in the given moment depends on values of concentration gradient (thermodynamic force) in the same point and in the same moment neglecting inertia of particles [59–61]. The simplest generalization of the transport process which removes this deficiency considers the time-delayed relations between flux and concentration gradient is given by [62–65]:

$$j(x,t)+\tau\frac{\partial j(x,t)}{\partial t}=-\mathrm{D}\frac{\partial\rho(x,t)}{\partial x} \tag{4}$$

where $\tau$ is inertial relaxation time [57,58].

The modified Fick's first law (Eq.4) and the continuity equation, Eq.2, give, in turn, a transport equation of hyperbolic type with a finite velocity of disturbance propagation, $v=\sqrt{D/\tau}$ [37,38,57–65]:

$$\frac{\partial\rho(x,t)}{\partial t}+\tau\frac{\partial^2\rho(x,t)}{\partial t^2}=D\frac{\partial^2\rho(x,t)}{\partial x^2} \tag{5}$$

The time-delayed flux and finite propagation speed concepts of transfer processes are the subject of interest in numerous papers especially in the theory of heat conduction where flux time-delayed hyperbolic transport theory is used for explanation of non-Fourier effects [66–74]. Generally, non-local flux can be described by [75–77].

$$j(x,t+\tau)=-\mathrm{D}\frac{\partial\rho(x,t)}{\partial x} \tag{6}$$

It is important to note that time-delayed constitutive relations (Eq.6, Eq.4) are in accordance with Second Law of Thermodynamic [57,58,65]. Such relations, in combination with conservation laws, lead to hyperbolic transport models that include two important properties of transport processes: the finite speed and non-locality i.e., multiple time scale nature of the out-of –thermodynamic equilibrium propagation [26,75–77]. On the other hand, they describe particle motion as Brownian and could not capture anomalous diffusion effects in highly heterogeneous systems such as skin. Recently, fractional models have been suggested for investigation of anomalous transport processes in micro scale heterogeneous systems [36–38].

A fractional order differential calculus is a generalization of the integer order integral and derivative to real or even complex order [78,79]. This idea first emerged at the end of the seventeenth century and has been developed in the area of mathematics throughout the eighteenth and nineteenth centuries in the works of, for example, Liouville, Riemann, Cauchy, Abel, Grünwald and many others [78,79]. There are three main definitions of the fractional order integrals, derivatives, and differences: Riemann–Liouville, Caputo-Fabrizio and Grünwald–Letnikov [78–80]. Some others are also present in the literature but are rarely used in applications [80]. More recently, by the end of the twentieth century, it turned out that some physical phenomena are modeled more accurately when fractional calculus is used [81]. Typical examples of the use of fractal derivatives can be found in physics and mathematics [19–21,81–85], in bioengineering [86], in geophysics [87], in polymers physics [88], etc. Tateishi et al. [80] recently described how the diffusion in complex systems can be accurately addressed with fractional time-derivative operator.

In this section, the Riemann–Liouville definition of fractional derivative is used [36,37]:

$$\frac{\partial^\nu f(x,t)}{\partial t^\nu}=\begin{cases}\dfrac{1}{\Gamma(1-\nu)}\dfrac{\partial}{\partial t}\displaystyle\int_0^t\frac{f(x,\mathrm{t}')}{(t-t')^\nu}dt' & 0<\nu<1\\[2ex] \dfrac{1}{\Gamma(-\nu)}\dfrac{\partial}{\partial t}\displaystyle\int_0^t\frac{f(x,\mathrm{t}')}{(t-t')^{1+\nu}}dt' & \nu<0\end{cases} \tag{7}$$

where $\Gamma(1-\nu)$and $\Gamma(-\nu)$) are the Euler Gamma functions and $\nu$ the fractional order with $\nu\in[0,1]$. The time derivative of fractional order of $\nu$ of $f(x,t)$is made as a weighted mean of the first derivative in the time interval [0, $t$]. The value of that first derivative at the time $t_1$ far apart from $t$ is given smaller weight than those closer in time to $t$. The further in time from particular $t$, the smaller the derivative associated weight. In other words, as time goes by the effect of past is fading away. The initial conditions for the fractional order differential equations with the Riemann-Liouville derivatives are in the same form as for the integer order differential equations.

The Laplace transform method is used often for solving engineering problems. The formula for the Laplace transform of the fractional derivative Eq.7 has the form [36,37].

$$\int_0^\infty e^{-st}\frac{\partial^\nu f(x,t)}{\partial t^\nu}dt=s^\nu\overline{F}(s)-\sum_{k=0}^{n-1}s^{\nu-k}f^{(k)}(0) \tag{8}$$

By phenomenological introduction of fractional derivatives into non-local constitutive equation, Eq.6, non-local fractional constitutive relation is obtained

$$j(x,t+\tau)=-\mathrm{D}_\gamma\frac{\partial^{1-\gamma}}{\partial t^{1-\gamma}}\frac{\partial\rho(x,t)}{\partial x} \tag{9}$$

where $\mathrm{D}_\gamma$ is generalized diffusion coefficient and $\left(\partial^{1-\gamma}\partial\rho(x,t)\right)/\left(\partial t^{1-\gamma}\partial x\right)$ is generalized thermodynamic force, which are the cause of anomalous diffusive behavior [36,37]. The fractional derivative of concentration gradient order of $\nu=1-\gamma$ is defined by Eq.7, where $\gamma$ is anomalous diffusive exponent.

By expanding the left-hand side of the Eq. 9 to the first power, an approximate constitutive relation is obtained that takes into account the delayed flux:

$$j(x,t)+\tau\frac{\partial j(x,t)}{\partial t}=-\mathrm{D}_\gamma\frac{\partial^{1-\gamma}}{\partial t^{1-\gamma}}\frac{\partial\rho(x,t)}{\partial x} \tag{10}$$

By combining Eq.(2) (continuity equation) and Eq.(10), the delayed anomalous fractional diffusion model is obtained:

$$\frac{\partial\rho(x,t)}{\partial t}+\tau\frac{\partial^2\rho(x,t)}{\partial t^2}=\mathrm{D}_\gamma\frac{\partial^{1-\gamma}}{\partial t^{1-\gamma}}\frac{\partial^2\rho(x,t)}{\partial x^2} \tag{11}$$

The same equation was proposed in the paper [37], where it was called the GCEIII model of anomalous diffusion.

Analysis of Eqs. (10)–(11) shows that for $\tau=0$ (non-delayed transport equation), and $0<\gamma<1$ it reduces to the standard subdiffusion model [36–38] while for $\gamma>1$ it reduces to superdiffusion model. The normal diffusion is characterized by $\gamma=1$ and $\tau=0$. For $\tau>0$, Eq. (11) is expected to predict different diffusion behavior on a time scale larger and smaller than $\tau$ and consequently at frequency scale smaller and larger than inverse $\tau$ similar to the classical hyperbolic equation [61,62,68,70], which is in accordance with experimental observations of mass transport [46–52].

In this paper, all further considerations of drug delivery across skin barrier are based on the model given by Eqs. (10) and (11).

## 3. Drug delivery across skin membrane

It is supposed that the transport of drugs, in a donor layer (DL) (patch or vehicle), is governed by Fick's laws of diffusion (given by Eqs. (1)–(3)), while the transport across the skin barrier (SC) is described by generalized fractional diffusion equations and non-local flux, described by Eqs. (10), (9), respectively. The concentration and flux profiles in the donor layer ($l_a\le x\le 0$, see Fig. 2), $\rho_1(x,t)$, $j_1(x,\mathrm{t})$ and in the skin barrier, SC, ($0\le x\le l_b$,see Fig. 2) $\rho_2(x,t)$, $j_2(x,\mathrm{t})$ are described by the two systems of partial differential equation.

For DL layer, $l_a\le x\le 0$, concentration profile and flux are described by classical diffusion theory:

$$\frac{\partial\rho_1(x,t)}{\partial t}=D_1\frac{\partial^2\rho_1(x,t)}{\partial x^2} \tag{11a}$$

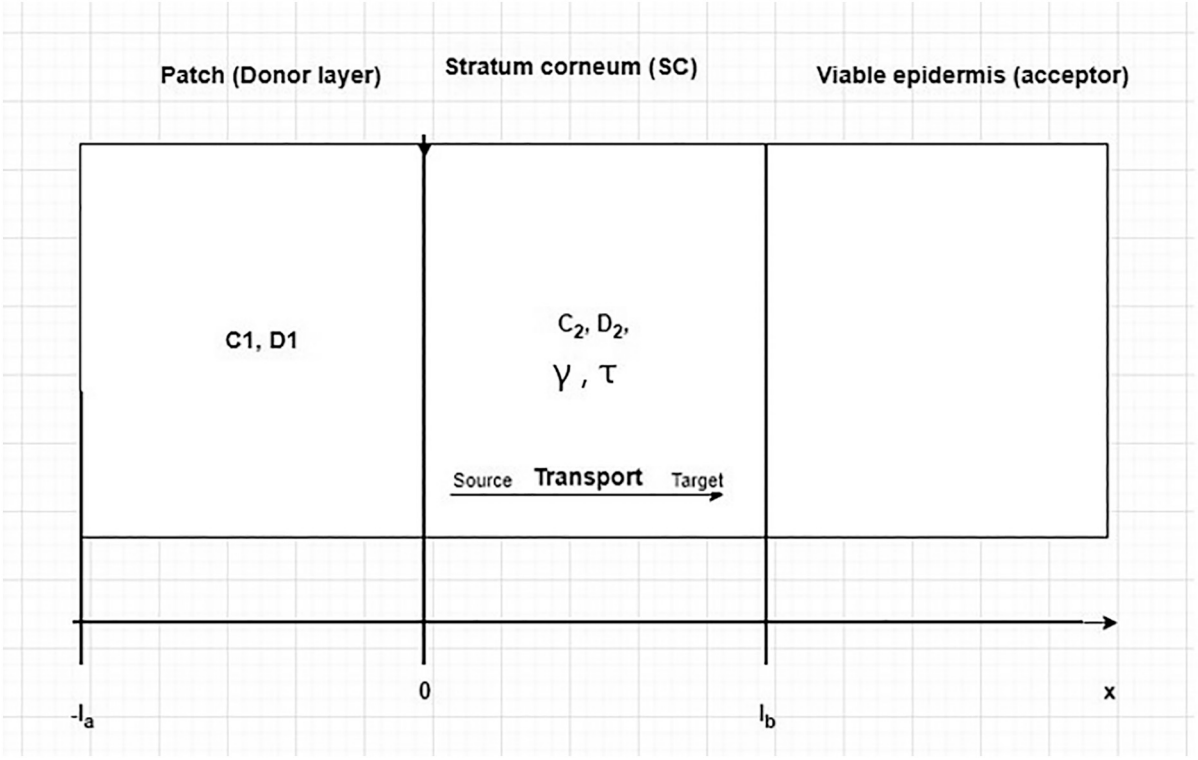


**Fig. 2.** Geometry of the problem. Patch with active substance and stratum corneum (SC) have sharp junction; each layer (donor layer and SC) has their concentration ($C_1$ and $C_2$ respectively) and diffusion coefficient ($D_1$ and $D_2$ respectively). Due to micro-scale heterogeneity of SC, the drug transport across skin barrier is described by two additional properties: anomalous diffusive exponent $\gamma$ and relaxation time $\tau$. On the right hand side, we can see viable epidermis layer that is considered to be a receiver or acceptor of mass transport later in the process once drug penetrates the skin.

$$j_1(x,t) = -\mathrm{D}_1\frac{\partial\rho_1(x,t)}{\partial x} \tag{11b}$$

For SC layer,$0 \le x \le l_b$, concentration profile and flux are described by generalized theory that includes anomalous diffusion and delayed flux across heterogeneous skin layer:

$$\frac{\partial\rho_2(x,t)}{\partial t}+\tau\frac{\partial^2\rho_2(x,t)}{\partial t^2} = \mathrm{D}_{2\gamma}\frac{\partial^{1-\gamma}}{\partial t^{1-\gamma}}\frac{\partial^2\rho_2(x,t)}{\partial x^2} \tag{12a}$$

$$j_2(x,t)+\tau\frac{\partial j_2(x,t)}{\partial t} = -\mathrm{D}_{2\gamma}\frac{\partial^{1-\gamma}}{\partial t^{1-\gamma}}\frac{\partial\rho_2(x,t)}{\partial x} \tag{12b}$$

In above equations Eqs. (11)–(12) with $D_1$ [$m^2$/s] is denoted the drug diffusion coefficient in the DL, $D_2$ [$m^2/s\gamma$] is generalized drug-diffusion coefficients in the SC layer, and $\tau$[s] is relaxation time (delayed time of flux in relation to gradient of concentration into skin barrier).

Assuming that the membrane is initially free of drug and that the drug is uniformly distributed within the donor layer, the following initial conditions hold [1]:

$$\rho_1(x,0) = C_0 h(t) \tag{13a}$$

$$\rho_2(x,0) = 0 \tag{13b}$$

$$\frac{\partial\rho_2(x,\mathrm{t})}{\partial t}|_{t=0} = 0 \tag{13c}$$

where $C_0$ is the initial drug concentration in the donor layer and $h(t)$ is Heaviside's function.

Eqs. (11)–(12) are subject to the following boundary conditions [1]:

$$j_1(x=-l_a,\mathrm{t}) = 0 \tag{14a}$$

$$\rho_2(x=l_b,\mathrm{t}) = 0 \tag{14b}$$

Eq. (14a) is a zero-flux boundary condition, which accounts for the absence of drug transport from the atmosphere into/out of the donor layer; Eq. (14b) refers to a perfect sink condition assumed in the case of a highly diluted reservoir (viable epidermis). A perfect sink condition is valid in the context of clinical applications because the medicament diffusing through the skin is being constantly removed by blood circulation.

It is assumed that there is flux continuity condition at the donor-membrane (DL/SC) boundary:

$$j_1(x=0,\mathrm{t}) = j_2(x=0,\mathrm{t}) \tag{15a}$$

and discontinuity of concentration at donor-membrane heterointerface (DL/SC) described by partition coefficient, $k_m$ (1)

$$\rho_1(x=0,\mathrm{t}) = k_m\rho_2(x=0,\mathrm{t}) \tag{15b}$$

The interface condition given by eq. (15b), the so-called partition condition [89,90], maintains a discontinuity between the solute concentration at the interface, with the partition coefficient $k_\mathrm{m}$ varying depending on the type of drug and solvent [1,91]. Such an interface condition can be understood as a more general form of the perfect contact condition, which is described by $k_\mathrm{m} = 1$. The partition interface condition is common in applications such as analyte transport in porous media [89] and drug release from multilayer capsules [1,90–91].

Following the paper [1], the normalization of variables results in the following relationships.

$$u_i(x,t) = \frac{\rho_i(x,t)}{C_0}, q_i(x,t) = \frac{j_i(x,t)}{C_0}, i = 1,2 \tag{16a}$$

$$\chi_1 = \frac{x}{l_a}, -l_a \le x \le 0, \chi_2 = \frac{x}{l_a}, 0 \le x \le l_b \tag{16b}$$

$$p = \frac{D_2}{l_b^2}, \eta = pt, T = p\tau \tag{16c}$$

The system of partial differential equations (PDEs), given by Eqs. (11)–(12), in terms of normalized variables becomes:

$$\frac{\partial u_1(\chi_1,\eta)}{\partial \eta} = \alpha \frac{\partial^2 u_1(\chi_1,\eta)}{\partial {\chi_1}^2} \tag{17a}$$

$$q_1(\chi_1,\eta) = -a_1 \frac{\partial u_1(\chi_1,\eta)}{\partial \chi_1} \tag{17b}$$

for $-1 \le \chi_1 \le 0$ and

$$\frac{\partial u_2(\chi_2,\eta)}{\partial \eta} + T\frac{\partial^2 u_2(\chi_2,\eta)}{\partial \eta^2} = p^{1-\gamma}\frac{\partial^{1-\gamma}}{\partial \eta^{1-\gamma}}\frac{\partial^2 u_2(\chi_2,\eta)}{\partial {\chi_2}^2} \tag{18a}$$

$$q_2(\chi_2,\eta) + T\frac{\partial q_2(\chi_2,\eta)}{\partial \eta} = -a_2 p^{1-\gamma}\frac{\partial^{1-\gamma}}{\partial \eta^{1-\gamma}}\frac{\partial u_2(\chi_2,\eta)}{\partial \chi_2} \tag{18b}$$

for $0 \le \chi_2 \le 1$.

The normalized initial and boundary conditions are given by following expressions:

$$u_1(\chi_1,\eta=0) = h(t), u_2(\chi_2,\eta=0) = 0, \frac{\partial u_2(\chi_2,\eta)}{\partial \eta}|_{\eta=0} = 0 \tag{19}$$

$$q_1(\chi_1 = -1,\eta) = 0 \tag{20a}$$

$$u_2(\chi_2 = 1,\eta) = 0 \tag{20b}$$

while normalized conditions at hetreointerfaces (Eq. 14) become:

$$q_1(\chi_1 = 0,\eta) = q_2(\chi_2 = 0,\eta) \tag{21a}$$

$$u_1(\chi_1 = 0,\eta) = k_m u_2(\chi_2 = 0,\eta) \tag{21b}$$

In the expressions given by Eqs. (17)–(18), the following nondimensional replacements have been introduced:

$$\alpha = \frac{D_1 l_b^2}{D_2 l_a^2} = \frac{1}{p}\frac{D_1}{l_a^2}, \beta = \frac{a_2}{a_1} \tag{22}$$

where coefficients:

$$a_1 = \frac{D_1}{l_a} \text{ and } a_2 = \frac{D_2}{l_b} \tag{23}$$

have a dimension of speed [m/s].

An analytical solution may be obtained by applying Laplace transform methods [92], with Laplace transform of fractional derivative given by Eq.8. This transform converts the systems of PDEs, Eqs.(17)–(18) into a system of linear ordinary differential equations in complex domain as follows:

$$\frac{d^2\overline{U}_1(\chi_1,s)}{d{\chi_1}^2} - \overline{\sigma}_1\overline{U}_1(\chi_1,s) = -\frac{1}{s\alpha} \tag{24a}$$

$$\overline{Q}_1(\chi_1,s) = -\frac{1}{\overline{\sigma}_1\overline{Z}_1}\frac{d\overline{U}_1(\chi_1,s)}{d\chi_1} \tag{24b}$$

for $-1 \le \chi_1 \le 0$, and

$$\frac{d^2\overline{U}_2(\chi_1,s)}{d{\chi_2}^2} - \overline{\sigma}_2\overline{U}_2(\chi_2,s) = 0 \tag{25a}$$

$$\overline{Q}_2(\chi_2,s) = -\frac{1}{\overline{\sigma}_2\overline{Z}_2}\frac{d\overline{U}_2(\chi_2,s)}{d\chi_2} \tag{25b}$$

for $0 \le \chi_2 \le 1$.

In Eqs. (24)–(25), the complex coefficients of propagation $\overline{\sigma}_i$ and complex impedance $\overline{Z}_i$. $i = 1,2$ are given by.

$$\overline{\sigma}_1 = \sqrt{\frac{s}{\alpha}}, \overline{Z}_1 = \frac{1}{a_1}\sqrt{\frac{\alpha}{s}} = \frac{1}{a_1}\frac{1}{\overline{\sigma}_1} \tag{26}$$

in the DL and

$$\overline{\sigma}_2 = \sqrt{\frac{s^\gamma(1+Ts)}{p^{1-\gamma}}}, \overline{Z}_2 = \frac{1}{a_2}\frac{\overline{\sigma}_2}{s} \tag{27}$$

in the skin barrier (SC layer).

With s is denoted complex frequency, $s = \sqrt{-1}\Omega$, where $\Omega$ is normalized angular frequency.

Boundary conditions in complex domain become:

$$\overline{Q}_1(-1,s) = 0, \overline{U}_1(1,s) = 0 \tag{28}$$

and conditions at heterointerface DL/SC become:

$$\overline{Q}_1(0,s) = \overline{Q}_2(0,s) \tag{29a}$$

$$\overline{U}_1(0,s) = k_m\overline{U}_2(0,s) \tag{29b}$$

By solving the system of linear ordinary differential equations in complex domain, Eqs.24–25 with boundary conditions Eqs. 28 and conditions at heterointerface Eqs.29, the spectral functions of concentrations are obtained:

$$\overline{U}_1(\chi_1,s) = \overline{U}_{1L}cosh[\overline{\sigma}_1(1+\chi_1)] - \frac{1}{s^2}[cosh[\overline{\sigma}_1(1+\chi_1)] - 1] \tag{30}$$

$$\overline{U}_2(\chi_2,s) = \overline{Q}_{2D}sinh[\overline{\sigma}_2(1-\chi_2)] \tag{31}$$

The complex constants $\overline{U}_{1L}$ and $\overline{Q}_{2D}$, obtained from conditions at heterointerface, Eqs. 29, are given by:

$$\overline{U}_{1L} = \frac{2sinh(\overline{\sigma}_1/2)}{s^2}\frac{\overline{Z}_1cosh(\overline{\sigma}_2)sinh(\overline{\sigma}_1/2) + k_m\overline{Z}_2sinh(\overline{\sigma}_2)cosh(\overline{\sigma}_1/2)}{\overline{Z}_1cosh(\overline{\sigma}_2)cosh(\overline{\sigma}_1) + k_m\overline{Z}_2sinh(\overline{\sigma}_2)sinh(\overline{\sigma}_1)} \tag{32}$$

$$\overline{Q}_{2D} = \frac{sinh(\overline{\sigma}_1)}{s^2}\frac{1}{\overline{Z}_1cosh(\overline{\sigma}_2)cosh(\overline{\sigma}_1) + k_m\overline{Z}_2sinh(\overline{\sigma}_2)sinh(\overline{\sigma}_1)} \tag{33}$$

In the next section, we analyze the spectral functions of concentration profiles in the donor layer and in the skin barrier in dependence of anomalous diffusive exponent, partition coefficient between donor layer and membrane and flux delayed time.

The cumulative amount of drug that diffuses through the *stratum corneum (SC layer)* into the viable epidermis at any specific time is of interest when one analyzes the transport of drug. It provides information regarding the amount of drug that is being absorbed into the blood circulation. Hence, we calculate this quantity by following definition from [1].

$$M = -Al_bC_0\int_0^\eta q_2(1,\eta)d\eta \tag{34}$$

where $A$ is the area exposed to the dosing solution. By application of Laplace transform to Eq.34, the cumulative amount of drug in complex domain becomes.

$$\overline{M} = -Al_bC_0\frac{1}{s}\overline{Q}_{2D} \tag{35}$$

The maximal value of the cumulative amount of drug in complex domain is [1]:

$$\overline{M}_\infty = -Al_bC_0\frac{1}{s} \tag{36}$$

By normalization of cumulative amount of drug (Eq. (35)) to maximal value (Eq.36), we obtained

$$\overline{M}_n = \overline{Q}_{2D} \tag{38}$$

In further discussion, we analyzed the spectral function of $\overline{Q}_{2D}(s)$ in order to discuss the influence of anomalous diffusive exponent, partition coefficient and flux delayed time to the cumulative amount of drug.

## 4. Analyzes and discussion

For $\gamma = 1$ and $T = 0$, the derived model given by Eqs.30–33 is reduced to the spectral functions of concentration and cumulative amount of drug given in the paper [1]. For $T = 0$, $l_a = 0$, and $k_m = 1$ the derived spectral function of concentration in the skin barrier given by Eqs. 31, 33 is reduced to model given in [41–45]. This confirms the validity of the derived model.

In this section, we analyzed how $k_m$ (that describes drug solvent characteristic in the patch) and $\gamma$ (that describes micro-structural heterogeneity of skin barrier) affect the spectral functions of the concentration profile and cumulative amount of drug, when the flux delay time $\tau$ (that is the finite speed of propagation of the mass perturbation in the skin) is taken into account.

### 4.1. Concentration profile and its spectral function

Among the many functions that the skin has for the human body, one of its main functions is the regulation of the entry of foreign substances into the body. This barrier function of the skin has attracted great scientific interest due to its role in numerous pharmacological and toxicological studies including transdermal drug delivery [91]. The partition of the drug, defined as the concentration ratio between the vehicle and the skin barrier in equilibrium, depends on both the drug itself and the characteristics of the skin membrane [1]. The partition coefficient km of a chemical in the skin is an indicator of the maximum amount of that chemical that the skin can contain and may reflect the rate at which the chemical penetrates the skin and enters the systemic circulation. In this study, the partition coefficient km varies depending on the type of drug and solvent vehicle, while the parameters $\gamma$ and T govern the transport of the drug through the skin.

The developed mathematical model can predict the release profile for a range of $k_m$ values that is, for various types of drugs and patches [1,93–95].

In order to examine the influence of normalized delayed time $T$ and partition coefficient $k_m$, the spectral function of the concentration profile based on the model given by Eqs. 30–33, and the spectral functions of the concentration profile are shown in Fig. 3, for $T = 100$, $\gamma = 1$ and for two values of $k_m$: $k_m = 1e\text{-}4$ (Fig. 3a, 3b) and $k_m = 1$ (Fig. 3c, d).

As can be seen from Fig. 3, when delay time is taken into account, $T \neq 0$, the model predicts changes in the spectral function of concentration in both layers. For low frequencies (Fig. 3a, c and red lines in Fig. 3b, d), the concentration along the donor layer is practically constant, as predicted by the previous models, both for a small (Fig. 3a, b)

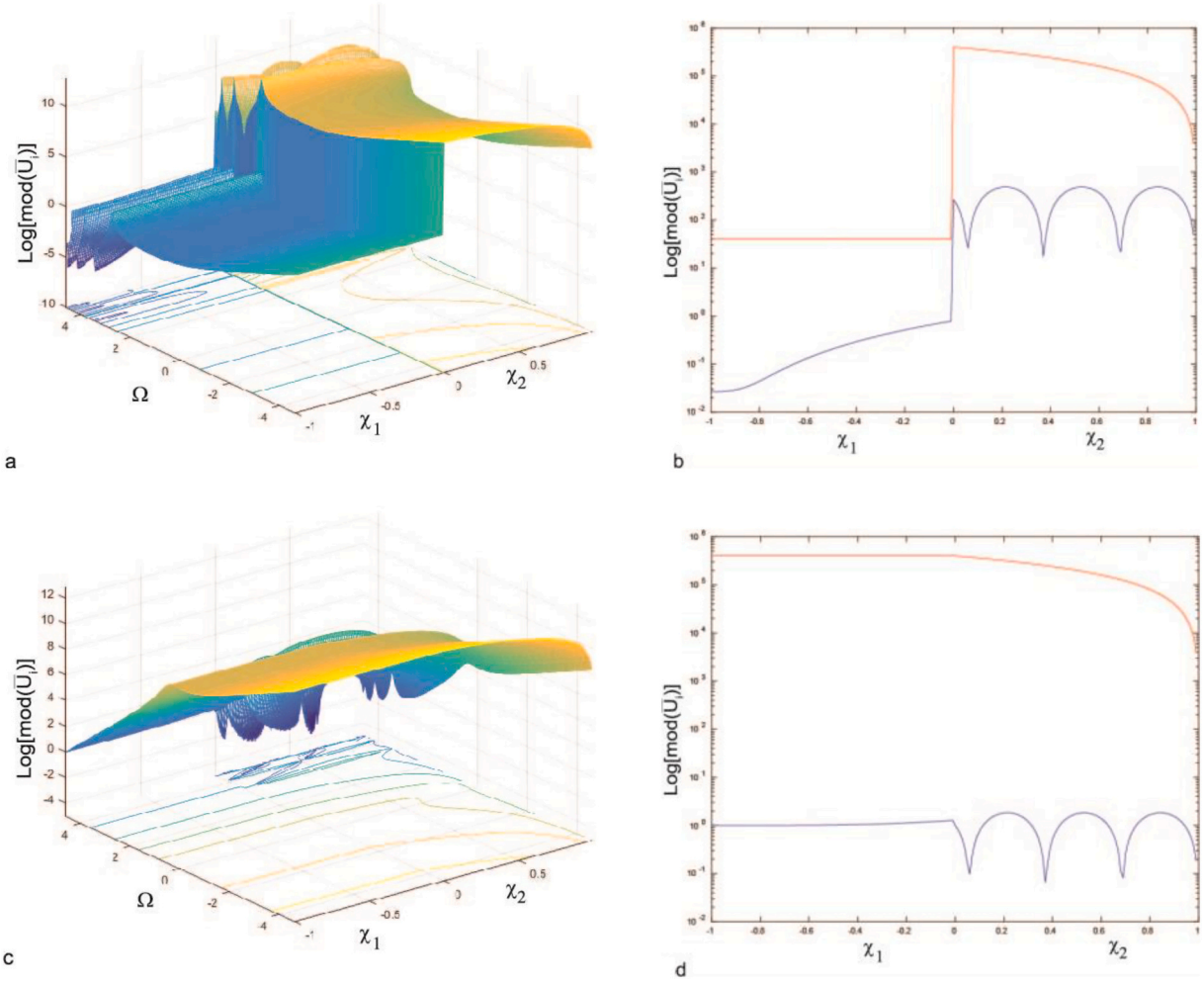


**Fig. 3.** The spectral functions of the concentration profile (left) and cross-sections for $\Omega = 10^{-2}$(red lines) and $\Omega = 10^{2}$ (blue lines) (right) based on the model given by Eq. 30–33, in the frequency range $10^{-2} \leq \Omega \leq 10^{2}$ for $\alpha = 6250, \beta = 0.00004$, $p = 0.1\ s^{-1}$ taken from [1] and for T = 100, $\gamma = 1$ as well as two values of $k_m$ a),b) $k_m = 1e\text{-}4$, c),d) $k_m = 1$. *(For interpretation of the references to colour in this figure legend, the reader is referred to the web version of this article.)*

and for $k_m$ equal to unity (Fig. 3c, d), but only for a small $k_m$ (Fig. 3a, b) there is a large jump in concentration noticeable on the DL/SC boundary. At high frequencies and small $k_m$, the concentration along the donor layer increases from the gas/DL boundary towards the DL/SC boundary. The steep concentration jump at the DL/SC boundary depends on the $k_m$. When the $k_m$ decreases, this jump is larger. It can be concluded that $k_m$ describes the ratio of affinity of the drug for the skin membrane and for the vehicle solvent. If these affinities are the same, partition coefficient is equal to unity, and there is no concentration discontinuity at a patch/skin interface.

Interesting changes in comparison to previous models can be observed in the spectral function of concentration along the SC (Fig. 3a-3d). At low frequencies, the concentration along the SC decreases monotonously from the DL/SC to the SC/VE boundary, and near this boundary the slope of the decrease increases significantly, as it is predicted by the previous models. However, at high frequencies, the spectral function shows oscillatory changes both along the frequency axis (Fig. 3a and c) and along the spatial axis (along the SC layer) (blue lines in Fig. 3b and d). From a physical point of view, the observed oscillatory changes can be interpreted as a *consequence of the change in the nature of transport at high frequencies*. Namely, for $\Omega > 1/T$ the perturbations propagate as damped waves, due to the finite propagation speed of the perturbation (or the inertial memory of the system as discussed in [61,71]), and the oscillatory changes are the consequence of resonances that occur when the integer multiple of half the wavelength of the perturbation becomes equal to the thickness of the layer through which the perturbation spreads. *Damping of the perturbation depends on the diffusion coefficient and the thickness of the sample, but also on the anomalous diffusion exponent* (Eq. 27). The partition coefficient does not affect either the damping or the period of these oscillatory changes.

Comparing Figs. 3a,b and 3c,d, it can be concluded that the partition coefficient affects the shape of the spectral function of the concentration in the donor layer and the value of the concentration along the SC layer increasing this concentration $k_m$ times if $k_m < 1$, at all frequencies.

In order to examine the influence of $T$ and the $\gamma$, the spectral function of the concentration profile based on the model given by eqs. 30–33, are shown in Fig. 4, for $k_m = 1$, $T = 100$, and for two values of $\gamma$: $\gamma = 0.1$ (Fig. 4a, 4b) and $\gamma = 0.9$ (Fig. 4c, d).

As can be seen from Fig. 4a - 4d, $\gamma$ does not affect the concentration profile along the donor layer in the entire frequency range. In this layer, the concentration is constant up to the DL/SC boundary, where there is a sudden but small jump down, which a loose depend on the size of the $\gamma$. At high frequencies, the concentration in the donor layer is lower than at low frequencies (blue and red lines in Fig. 4b and d). Therefore, the DL/SC heterointerface itself presents a *barrier* on which molecules accumulate, but the rate of diffusion expressed through the anomalous diffusion exponent $\gamma$ does not affect its capacitance.

In the SC layer, one can observe oscillatory changes in the spectral function of concentration at high frequencies, for high $\gamma$ (Fig. 4c and blue line in Fig. 4d), similarly as in previous Fig. 3a, c, blue lines in Fig. 3b, d, which are a consequence of the fact that the delayed time is different from zero, i.e. a consequence of the finite propagation speed of the mass

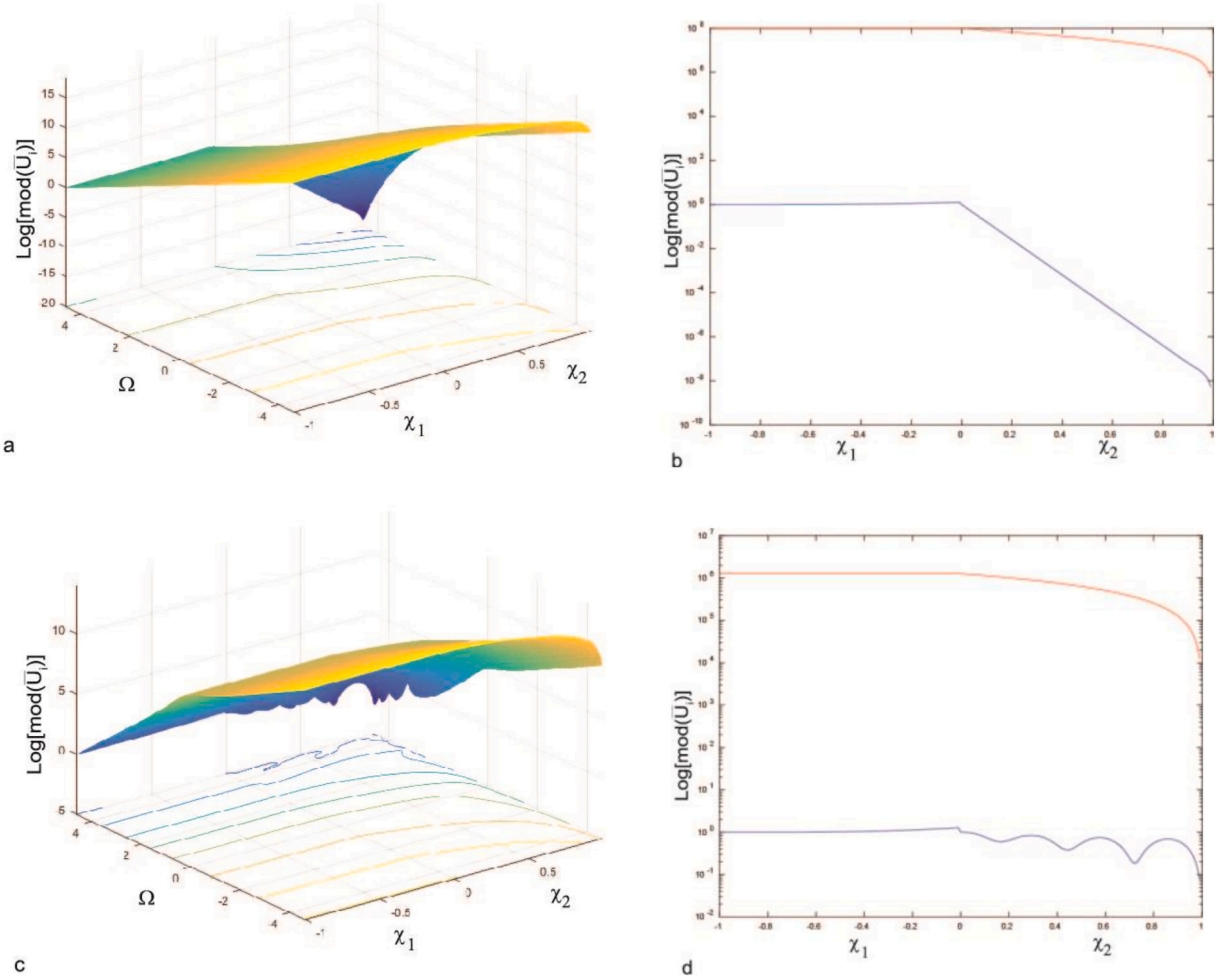


**Fig. 4.** The spectral functions of the concentration profile (left) and cross-sections for $\Omega = 10^{-2}$(red lines) and $\Omega = 10^2$ (blue lines) (right) based on the model given by Eq. 30–33, in the frequency range $10^{-2} \leq \Omega \leq 10^2$ for $\alpha = 6250, \beta = 0.00004$, $p = 0.1$ s$^{-1}$ taken from [1] and for $T = 100$, $k_m = 1$ as well as two values of $\gamma$ a,b) $\gamma = 0.1$, c,d) $\gamma = 0.9$. (For interpretation of the references to colour in this figure legend, the reader is referred to the web version of this article.)

perturbation and the inertia of the drug molecules. Anomalous diffusion exponent influences the attenuation of amplitude of damped wave inside the SC (Figs.3b,3d, blue lines) so that this attenuation is greater when the $\gamma$ is smaller. Effectively, when $\gamma$ decreases, both the diffusion length of the perturbation and its wavelength decrease (Eq.27), so that the oscillation frequency becomes higher and the oscillation amplitude decreases. For very small$\gamma$ oscillations are lost (blue line, Fig. 4b).

For a large$\gamma$ (close to unity), at high frequencies, there is a completely different concentration gradient along the SC in comparison to those at low frequencies (the blue lines in Fig. 4b and d). This influence on the concentration gradient in the SC is related to the influence of $\gamma$ on the impedance of the SC (Eq, 27). With an increase in$\gamma$, the capacitance of the SC layer increases, and the mismatch between the impedances of SC and DL decreases.

Comparing Figs. 4a,b and 4c,d, it can be concluded that the anomalous diffusive exponent affects the shape of the spectral function of the concentration in the SC layer and for parameter $\gamma \neq 1$, the value of the concentration at interface between donor layer and SC and within SC layer decreases.

In order to examine the influence of $T$ in more detail, the spectral functions of the concentration profile based on the model given by eqs. 30–33, are shown in Fig. 5, for $k_m = 1$, $\gamma = 0.8$ and for two values of $T$: $T = 1$ (Fig. 5a, 5b) and b) $T = 100$ (Fig. 5c, d).

As can be seen from Figs. 5 a-d, $T$ does not affect the shape of the concentration profile either in the donor layer or in the SC layer, at low frequencies. In the donor layer, at low frequencies, the concentration is practically constant up to the DL/SC boundary (red lines, Fig. 5b, d). At low frequencies, the concentration along the SC layer decreases monotonically with a large increase in slope near the SC/VE boundary (red lines, Fig. 5b, d). However, at high frequencies $T$ affects both the shape of concentration profile in the donor layer and the shape of concentration profile in the SC layer. In the donor layer, this influence of T is more pronounced for smaller T, where an increase in concentration along the DL and a sudden jump down at the DL/SC boundary is observed, where the slope of the increase decreases and the size of the jump increases with the increase in $T$ (blue lines, Fig. 5b, d). At high frequencies, greater than inverse $T$, the concentration profile along the SC shows oscillatory changes both along the frequency and along the spatial axis whose frequency decreasing with increasing T (Figs.5a, c, blue lines in Figs.5b, 5d). An increase in $T$ increases both the wavelength and the diffusion length of the mass perturbation for $\Omega > 1/T$. This means that an increase in $T$ shifts the frequency at which resonance occurs towards higher frequencies, simultaneously reducing the oscillation amplitudes.

Comparing Figs. 5a,b and 5c,d, it can be concluded that the flux delayed time affects the shape of the spectral function of the concentration in the SC layer and increase in $T$ steeply decreases the value of the concentration at interface between donor layer and SC and slows the decline along the SC layer.

Based on this analysis (blue lines in Fig. 5b, d), we can be conclude that $T$ affects the impedance of the SC layer, which can be seen from Eq.27, also. Namely, an increase in $T$, similar to an increase in $\gamma$ (Fig. 4) affects a decrease in the impedance of the SC layer and consequently

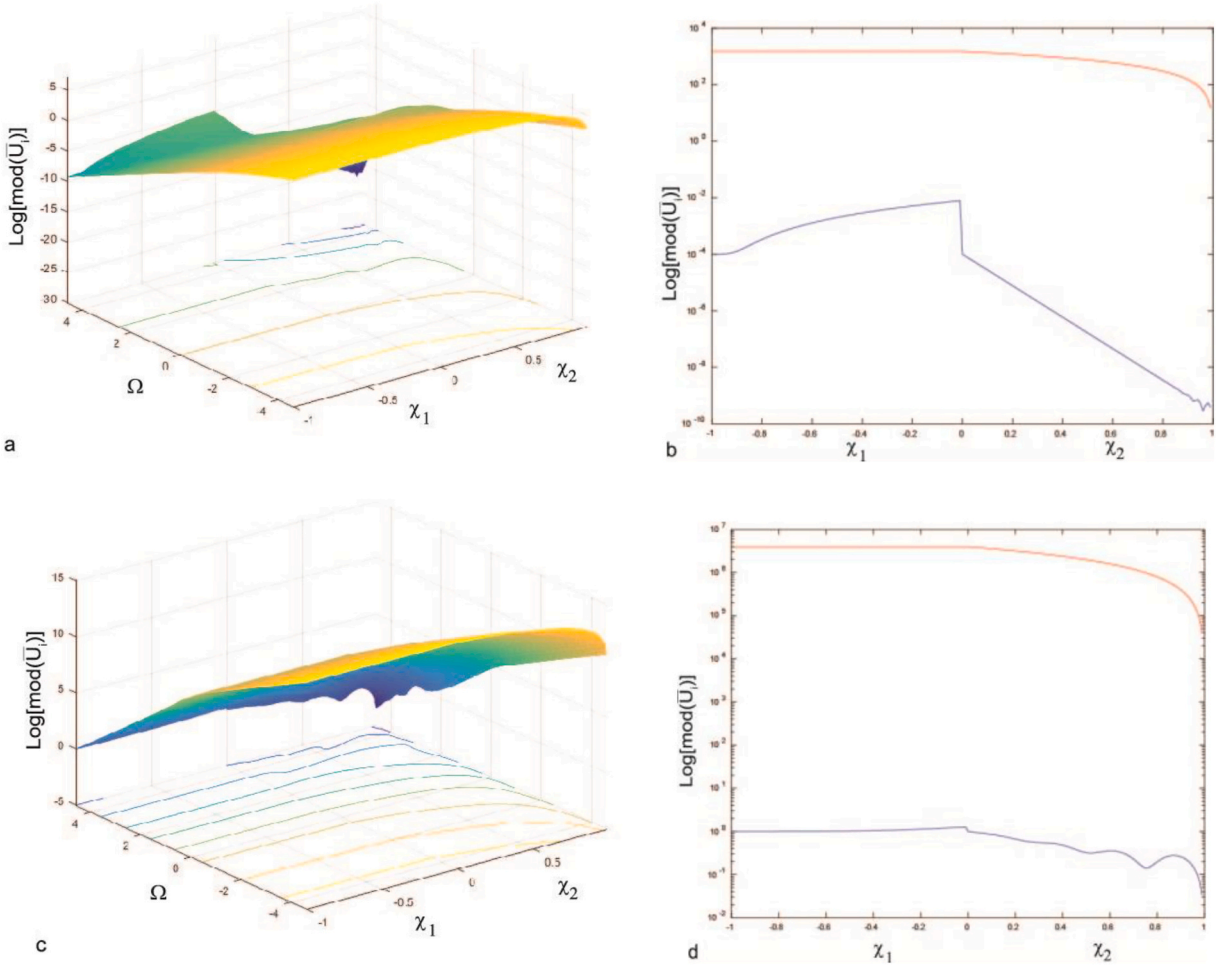


**Fig. 5.** The spectral functions of the concentration profile (left) and cross-sections for $\Omega = 10^{-2}$(red lines) and $\Omega = 10^{2}$ (blue lines) (right) based on the model given by Eq. 30–33, in the frequency range $10^{-2} \leq \Omega \leq 10^{2}$ for $\alpha = 6250, \beta = 0.00004$, $p = 0.1\ s^{-1}$ taken from [1] and for $\gamma = 0.8$, $k_m = 1$ as well as two values of $T$ a),b) $T = 1$, c),d) $T = 100$. (For interpretation of the references to colour in this figure legend, the reader is referred to the web version of this article.)

gives smaller mismatch between the impedances of DL and SC, so it is expected that this influence is also manifested in the cumulative flux.

### 4.2. The spectral function of the cumulative amount of drug

In this section, we analyzed how $k_m$ and $\gamma$ affect the spectral functions of the cumulative amount of drug, when the flux delay time $\tau$ is taken into account, based on the model given by Eqs. 38 and 33.

Fig. 6 shows how the anomalous diffusive exponent $\gamma$ affects the spectral function of the cumulative amount of the drug.

From Fig. 6a, for $\gamma \leq 0.5$, it is obvious that the cumulative amount of drug decreases monotonically if frequency increases, with the rate of decrease which increases when $\Omega > 1/T$. For $\gamma > 0.5$, the spectral function shows oscillatory changes in the amplitude of the cumulative amount of drug at $\Omega > 1/T$, with larger oscillations for higher $\gamma$ (Fig. 6a, blue line) and faster phase decay (Fig. 6b, blue line). In addition, the larger the $\gamma$, the higher cumulative amounts of the drug in the entire frequency range.

Fig. 7 shows how T affects the cumulative amount of drug.

As it can be seen from Fig. 7a and b the increase in the $T$ (decrease in the propagation speed of the perturbation) leads to the appearance of oscillatory behavior in both amplitudes and phases of the cumulative flux at frequencies$\Omega > 1/T$. These oscillations are consequence of the resonances in molecular density into SC, as it is discussed below the Fig. 3-5. Consequently, they can be observed in both, amplitudes and phases of cumulative flux at high frequencies$\Omega > 1/T$. It also means that there is change in the transport nature of perturbation: at low frequencies $\Omega < 1/T$ (that is, in long time limit, $t > T$) it is sub-diffusion transport while at high frequency $\Omega > 1/T$ (that is short time limit, $t < T$) there is damped wave propagation.

The parameter T influence to diffusion length and wavelength of perturbation, and consequently to magnitudes of oscillations, their periods, and characteristic frequency at which the first resonance appears. Besides, the smaller $T$ the lower level of cumulative amount of drug at all frequencies, similar to influence of $\gamma$. It can be explained by dependence of the SC layer impedance on $T$, Eq.27.

The conducted analyzes indicates that in a short time interval (of the order of magnitude of the T) from the moment of applying the patch, overshoots of saturation of cumulative amount of drug are occurring, while in a time interval that is much longer than $T$ the saturation cumulative flux is achieved more slowly. Also, there are oscillations around this value with an amplitude that depends not only on the delay time (propagation speed of the perturbation) but also on $\gamma$.

Fig. 8 shows how $k_m$ affects the cumulative amount of drugs if the time delay $T$ is large.

As can be seen from Fig. 8a, b $k_m$ affects the change in the rate of decline of the cumulative flux amplitudes and phases. With the decrease in $k_m$, the amplitudes of the cumulative flux decrease more slowly, especially at high frequencies, where the influence of $T$ comes to the fore. In addition, the increase in $k_m$, similarly to the decrease in $T$, affects the shift of the resonances towards higher frequencies (shorter time intervals). Unlike the influence of increases of $T$ and increase of $\gamma$ (Figs. 7 - 8), the increase in $k_m$ does not affect the magnitude of the cumulative flux at low frequencies,$\Omega < 1/T$ but affects the decrease of the cumulative flux at high frequencies, $\Omega > 1/T$.

If the drug has a higher affinity for the vehicle solvent than for membrane (high $k_{\mathrm{m}}$), the delivery rate is considerably slower at high frequencies or in short time limit, while in long time limit the influence of $k_{\mathrm{m}}$ to the partition of the drug can be ignored.

## 5. Conclusion

Derived model introduces time-delayed flux concept and consequently inertial relaxation time $\tau$ in mathematical description of particle transport processes across biological barrier to take into account its time-scale dependent nature. Besides, the model introduces anomalous diffusive exponent $\gamma$ to consider anomalous diffusive behavior of particle into highly heterogeneous media.

For $\gamma \neq 1$ and $\tau = 0$ the model is reduced to existing models that consider anomalous diffusive behavior but ignore time-scale dependent nature of particles transport. For $\gamma = 1$ and $\tau = 0$ the model is reduced to classical model of drug delivery across the skin barrier. It means that derived model represents a generalization of both types of existing models.

The analysis of the spectral functions of the concentration profile and the cumulative flux showed that micro-heterogeneity of the SC affects the occurrence of sub-diffusive drug transport at frequencies lower than inverse flux delay time, while at frequencies higher than that, resonant changes in concentration profile and oscillations of the spectral function of the cumulative flux are observed, which indicate the wave nature of the propagation of the perturbation at high frequencies, i.e. in the short time limit. This phenomenon is a consequence of taking into account the

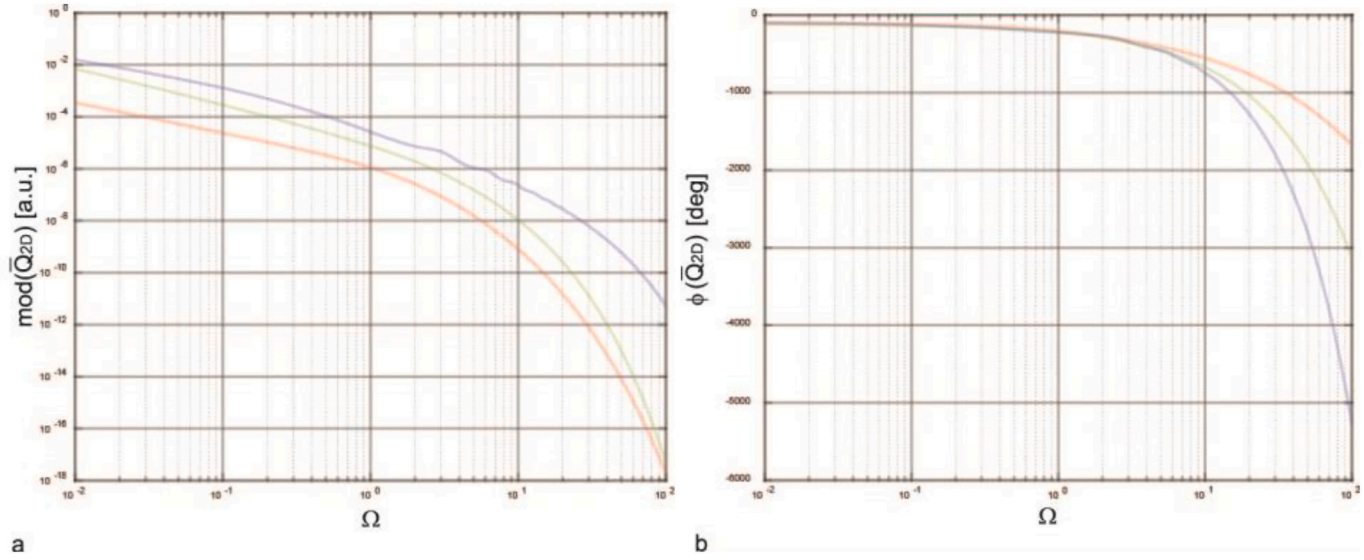


**Fig. 6.** Spectral function of cumulative amount of drugs for $\alpha = 6250, \beta = 0.00004.$, p = 0.1 $s^{-1}$, $k_m = 1$, T = 1, $\gamma = 0.1$(red lines), $\gamma = 0.5$ (green lines), and $\gamma = 0.9$ (blue lines). a)Amplitude characteristic of the cumulative amount of drug b) Phase characteristic of the cumulative amounts of the drug. (For interpretation of the references to colour in this figure legend, the reader is referred to the web version of this article.)

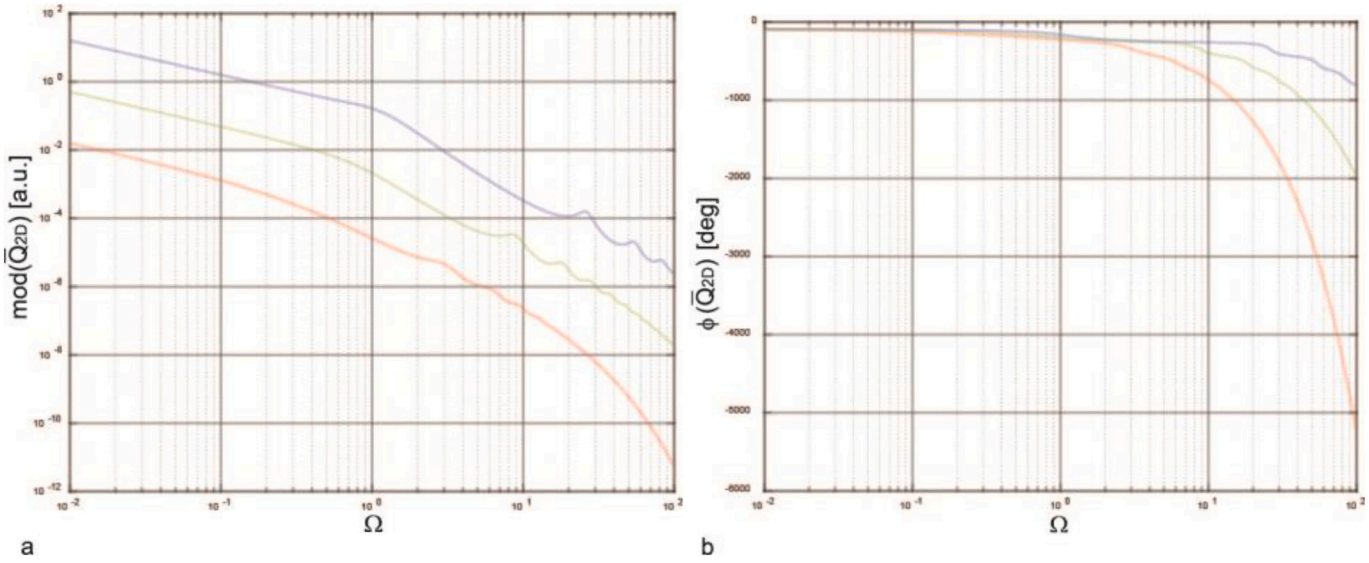


**Fig. 7.** Spectral function of cumulative amount of drugs for $\alpha = 6250$,$\beta = 0.00004$., p = 0.1 $s^{-1}$, $k_m = 1$, $\gamma = 0.9$, and three values of *T: T* = 1 (red line), T = 10 (green line), and T = 100 (blue line). a) Amplitude characteristic of the cumulative amount of drug; b) Phase characteristic of the cumulative amounts of the drug. (For interpretation of the references to colour in this figure legend, the reader is referred to the web version of this article.)

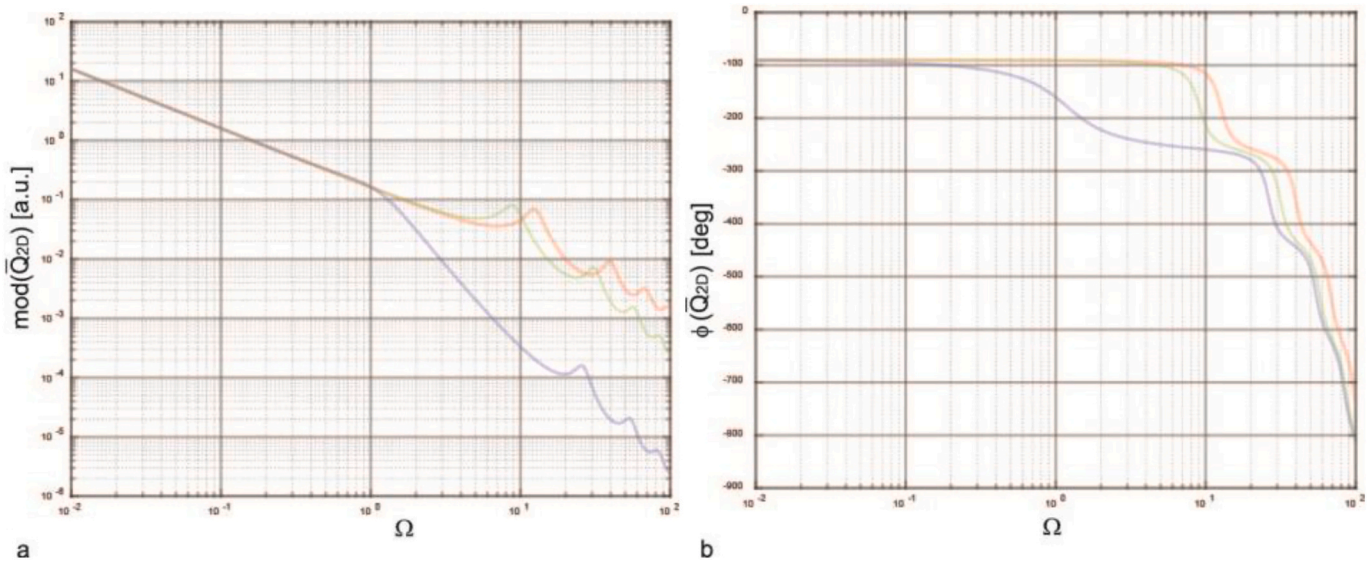


**Fig. 8.** Spectral function of cumulative amount of drugs for $\alpha = 6250$,$\beta = 0.00004$., p = 0.1 $s^{-1}$, $\gamma = 0.9$, T = 100, and three values of $k_m$: $k_m = 0.0001$ (red line), km==0.01 (green line), and $k_m = 1$ (blue line). A) amplitude characteristic of the cumulative amount of drug; b) Phase characteristic of the cumulative amounts of the drug. (For interpretation of the references to colour in this figure legend, the reader is referred to the web version of this article.)

non-locality of the flux, i.e. the *finite propagation speed of the perturbation*.

As the anomalous diffusion exponent is higher, the sub-diffusive properties are less pronounced in the low-frequency range (long-time limit), as well as the damping of the perturbation waves at high frequencies (short-time limit). The influence of this exponent on cumulative flux at low and high frequencies is of a different origin. At low frequencies, the anomalous diffusive exponent dominantly affects SC impedance and impedance mismatch between SC and DL. At high frequencies, $\Omega > 1/T$, this exponent dominantly affects diffusion length and wavelength of the perturbation transport.

The partition coefficient affects the cumulative flux as a time (frequency)-dependent impedance that describes the accumulation property of skin barrier (capacity) for given ratio of affinity of the drug for the skin membrane and for the vehicle solvent. The saturation value of the concentration along the SC layer also depends on this coefficient. It means that the adjustment of this coefficient should be done for various drug molecules (by permeation enhancer in vehicle solvent or by patch structure [91,95]) to control release concentration of drug and saturation cumulative amount of drug.

Accounting for the finite speed of propagation of the perturbation, i. e. the flux delay time, explains the experimentally observed phenomenon that the nature of the transport is different if it is observed on different time (frequency) scales. An increase in the delay time affects the increase of the perturbation wavelength and its diffusion length and leads to the *amplification of resonance amplitudes* in the concentration profile as well as in the spectral function of the cumulative amount of the drug. Based on these observations, it can be concluded that in a time interval of the order of the flux delay time overshoots of steady cumulative flux (saturation cumulative amount of the drug) are occurring and in long time limit the saturation cumulative flux is achieved more slowly

through oscillation around the equilibrium value with an amplitude that depends not only on the propagation speed of the perturbation, but also on the anomalous diffusion exponent. It is important to note that non-delayed models predict the asymptotic reaching of saturation (equilibrium cumulative flux) in the long-time limit, through asymptotic approaching to this value with a rate that increases with the increase of the anomalous diffusion exponent. It means that non-zero flux time delay may cause a larger cumulative amount of the drug than saturation value during long time interval what can have significant physiological implications. Therefore, the duration of drug administration through the skin should be estimated by considering non-zero flux delay in medical applications of patch with drug solution.

## CRediT authorship contribution statement

These authors equally contributed to this work.

## Declaration of competing interest

The authors declare that they have no known competing financial interests or personal relationships that could have appeared to influence the work reported in this paper.

## Data availability

Data will be made available on request.

## Acknowledgments

This work was supported by the Margit Weisheit and Parrotia Foundation support to Empa Material Science and Technology (MC) Swiss Federal Laboratories for Materials Science and Technology) at St. Gallen (Project Digital human avatars help customize transdermal pain therapy in real time) 2022/2023. SG received salary by the Ministry of Science, Technological Development and Innovation of the Republic of Serbia, contract number 451-03-47/2023-01/200017. We also want to thank Prof. Dr. Thijs Defraeye and Prof. Dr. René Michel Rossi for useful discussions and comments during writing of the paper.

## References

[1] Fernandes M, Simon L, Loney NW. Mathematical modeling of transdermal drug delivery systems: analysis and applications. J Membr Sci 2005;256:184–92. https://doi.org/10.1016/j.memsci.2005.02.018.
[2] Pontrelli G, de Monte F. A two-phase two-layer model for transdermal drug delivey and percutaneous adsorption. Math Biosci 2014;257:96–103. https://doi.org/10.1016/j.mbs.2014.05.001.
[3] Simon L. Repeated application of a transdermal patch: analytical solutions and optimal control of the delivery rate. Math Biosci 2007;209:593–607. https://doi.org/10.1016/j.mbs.2007.03.009.
[4] Jones JG, White KAJ, Delgado-Charro MB. A mechanicistic approach to modelling the formation of a drug reservoir in the skin. Math Biosci 2016;281:36–45. https://doi.org/10.1016/j.mbs.2016.08.007.
[5] Anissimov YG, Jepps OG, Dancik Y, Roberts MS. Mathematical and farmacokinetics modelling of epidermal and dermo transport processes. Adv Drug Deliv Rev 2013;65:169–90. https://doi.org/10.1016/j.addr.2012.04.009.
[6] Rim Jee E, Pinsky Peter M, van Osdol William W. Finite element modeling of coupled diffusion with partitioning in transdermal drug delivery. Ann Biomed Eng 2005;33(10):1422–38. https://doi.org/10.1007/s10439-005-5788-6.
[7] Naegel A, Wittum G. Detailed modelling of skin penetration: an overview. Adv Drug Deliv Reviews 2013;65:191–207. https://doi.org/10.1016/j.addr.2012.10.009.
[8] Jepps OG, Daneik Y, Anissimov YG, Roberts MS. Modeling the human skin barrier. Towards a better understanding of dermal adsorption. Adv Drug Deliv Rev 2013;65:152–68. https://doi.org/10.1016/j.addr.2012.04.003.
[9] Selzer Dominik, Neumann Dirk, Schaefer Ulrich F. Mathematical models for dermal drug absorption. Expert Opin Drug Metab Toxicol 2015;11(10):1–17. https://doi.org/10.1517/17425255.2015.1063615.
[10] Scher H, Montroll EW. Anomalous transit-time dispersion in amorphous solids. Phys. Rev. B 1975;12:2455. https://doi.org/10.1103/physrevb.12.2455.
[11] Schubert M, Preis E, Blakesley JC, Pingel P, Scherf U, Neher D. Mobility relaxation and electron trapping in a donor/acceptor copolymer. Phys Rev B 2013;87:024203. https://doi.org/10.1103/PhysRevB.87.024203.
[12] Chen KJ, Wang B, Granick S. Memoryless self-reinforcing directionality in endosomal active transport within living cells. Nature Mater 2015;14:589. https://doi.org/10.1038/nmat4239.
[13] Song MS, Moon HC, Jeon J-H, Park HY. Neuronal messenger ribonucleoprotein transport follows an aging Lévy walk. Nature Comm 2018;9:344. https://doi.org/10.1038/s41467-017-02700-z.
[14] Gupta S, de Mel JU, Perera RM, Zolnierczuk P, Bleuel M, Faraone A, et al. Dynamics of phospholipid membranes beyond thermal undulations. J. Phys. Chem. Lett. 2018;9:2956–60. https://doi.org/10.1021/acs.jpclett.8b01008.
[15] He W, Song H, Su Y, Geng L, Ackerson BJ, Peng HB, et al. Dynamic heterogeneity and non-Gaussian statistics for acetylcholine receptors on live cell membrane. Nat Commun 2016;7:11701. https://doi.org/10.1038/ncomms11701.
[16] Jeon J-H, Javanainen M, Martinez-Seara H, Metzler R, Vattulainen I. Protein crowding in lipid bilayers gives rise to non-Gaussian anomalous lateral diffusion of phospholipids and proteins. Phys Rev X 2016;6:021006. https://doi.org/10.1103/PhysRevX.6.021006.
[17] Wu H, Schwartz DK. Nanoparticle tracking to probe transport in porous media. Acc Chem Res 2020;53(10):2130–9. https://doi.org/10.1021/acs.accounts.0c00408.
[18] Wu H, Wang D, Schwartz DK. Connecting hindered transport in porous media across length scales: from single-pore to macroscopic. J Phys Chem Lett 2020;11(20):8825–31.
[19] Somer A, Popovic MN, da Cruz GK, Novatski A, Lenzi EK, Galovic SP. Anomalous thermal diffusion in two-layer system: the temperature profile and photoacoustic signal for rear light incidence. Int J Therm Sci 2022;179:107661. https://doi.org/10.1016/j.ijthermalsci.2022.107661.
[20] Somer A, Galovic S, Lenzi EK, Novatski A, Djordjevic K. Temperature profile and thermal piston component of photoacoustic response calculated by the fractional dual-phase-lag heat conduction theory. International Journal of Heat and Mass Transfer 2023;203:123801. https://doi.org/10.1016/j.ijheatmasstransfer.2022.123801.
[21] Koh Yee Rui, Shirazi-HD MohammadAli, Vermeersch Bjorn, Mohammed Amr MS, Shao Jiayi, Pernot Gilles, et al. Quasi-ballistic thermal transport in Al0.1Ga0.9N thin film semiconductors. Appl Phys Lett 2016;109:243107. https://doi.org/10.1063/1.4972186.
[22] Metzler Ralf, Rajyaguru Ashish, Berkowitz Brian. Modelling anomalous diffusion in semi-infinite disordered systems and porous media. New J Phys 2022;24:123004. https://doi.org/10.1088/1367-2630/aca70c.
[23] Sposini Vittoria, Krapf Diego, Marinari Enzo, Sunyer Raimon, Ritort Felix, Taheri Fereydoon, et al. Towards a robust criterion of anomalous diffusion. Communication Physics 2022;5(1):305. https://doi.org/10.1038/s42005-022-01079-8.
[24] Jeon Jae-Hyung, Javanainen Matti, Martinez-Seara Hector, Metzler Ralf, Vattulainen Ilpo. Protein crowding in lipid bilayers gives rise to non-Gaussian anomalous lateral diffusion of phospholipids and proteins. PHYSICAL REVIEW X 2016;6:021006. https://doi.org/10.1103/PhysRevX.6.021006.
[25] Fernandez Amanda Dıez, Charchar Patrick, Cherstvy Andrey G, Metzler Ralf, Finnis Michael W. The diffusion of doxorubicin drug molecules in silica nanoslits is non-Gaussian, intermittent and anticorrelated. Phys.Chem.Chem.Phys. 2020;22:27955. https://doi.org/10.1039/d0cp03849k.
[26] Liang Yingjie, Wang Wei, Metzler Ralf. Anomalous diffusion, non-Gaussianity, and nonergodicity for subordinated fractional Brownian motion with a drift. arXiv:2302.04872v1 [cond-mat.stat-mech] 2023. 9 Feb:1-10.
[27] Furth R, editor. Albert Einstein: Investigations on the theory of the Brownian movement. New York, NY: Dover; 1956.
[28] von Smoluchowski M. Zur kinetischen Theorie der Brownschen Molekularbewegung und der Suspensionen. Ann Phys (Leipzig) 1906;21, 756. https://doi.org/10.1002/andp.19063261405.
[29] Nordlund I. A new determination of Avogadro's number from Brownian motion of small mercury spherules. Z Phys Chem 1914;87:40.
[30] Hofling F, Franosch T. Anomalous transport in the crowded world of biological cells. Rep Prog Phys 2013;76:046602. https://doi.org/10.1088/0034-4885/76/4/046602.
[31] Norregaard K, Metzler R, Ritter C, Berg-Sorensen K, Oddershede L. Manipulation and motion of organelles and single molecules in living cells. Chem Rev 2017;117:4342. https://doi.org/10.1021/acs.chemrev.6b00638.
[32] Scher H, Shlesinger MF, Bendler JT. Time-scale invariance in transport and relaxation. Phys. Today 1991;44(1):26. https://doi.org/10.1063/1.881289.
[33] Barkai E, Garini Y, Metzler R. Strange kinetics of single molecules in living cells. Phys Today 2012;65(8):29. https://doi.org/10.1063/PT.3.1677.
[34] Metzler R, Klafter J. The random walk's guide to anomalous diffusion: a fractional dynamic approach. Phys Rep 2000;339(1):1–77. https://doi.org/10.1016/S0370-1573(00)00070-3.
[35] Bouchaud J-P, Georges A. Anomalous diffusion in disordered media: statistical mechanisms, models and physical applications. Phys Rep 1990;195(4–5):127–293. https://doi.org/10.1016/0370-1573(90)90099-N.
[36] Metzler R, Nonnenmacher TF. Fractional diffusion: exact representations of spectral functions. J Phys A: Math Gen 1997;30:1089–93. https://doi.org/10.1088/0305-4470/30/4/011.
[37] Comptey Albert, Metzlerz Ralf. The generalized Cattaneo equation for the description of anomalous transport processes. J. Phys. A: Math. Gen. 1997;30:7277–89. https://doi.org/10.1088/0305-4470/30/21/006.
[38] Korabel N, Klages R, Chechkin AV, Sokolov IM, Gonchar VYu. Fractal properties of anomalous diffusion in intermittent maps. PHYSICAL REVIEW E 2007;75:036213. https://doi.org/10.1103/PhysRevE.75.036213.
[39] Kiryakova VS. Generalized fractional Calculus and applications. Longman Scientific and Technical: Harlow; 1994.

[40] Cesarone F, Caputo M, Camettia C. Memory formalism in the passive diffusion across, highly heterogeneous systems. J Membr Sci 2005;250:79–84. https://doi.org/10.1016/j.memsci.2004.10.018.

[41] Dokoumetzidis A, Macheras P. Fractional kinetics in drug absorption and disposition processes. J Pharmacokinet Pharmacodyn 2009;36:165–78. https://doi.org/10.1007/s10928-009-9116-x.

[42] Popovic JK, Atanackovic MT, Pilipovic AS, Rapaic MR, Pilipovic S, Atanackovic TM. A new approach to the compartmental analysis in pharmacokinetics: fractional time evolution of diclofenac. J Pharmacokinet Pharmacodyn 2010;37:119–34. https://doi.org/10.1007/s10928-009-9147-3.

[43] Dokoumetzidis A, Magin R, Macheras P. Fractional kinetics in multi-compartmental systems. J Pharmacokinet Pharmacodyn 2010;37:507–24. https://doi.org/10.1007/s10928-010-9170-4.

[44] Caputo M, Cametti C, Ruggero V. Time and spatial concentration profile inside a membrane by means of a memory formalism. Physica A 2008;387:2010–8. https://doi.org/10.1016/j.physa.2007.11.033.

[45] Caputo M, Cametti C. Diffusion through skin in the light of a fractional derivative approach: progress and challenges. J Pharmacokinet Pharmacodyn 2021;48:3–19. https://doi.org/10.1007/s10928-020-09715-y.

[46] Saxton MJ, Jacobson K. Single-particle tracking: applications to membrane dynamics. Annu Rev Biophys Biomol Struct 1997;26:373–99. https://doi.org/10.1146/annurev.biophys.26.1.373.

[47] Wirtz D. Particle-tracking microrheology of living cells: principles and applications. Annu Rev Biophys 2009;38:301–26. https://doi.org/10.1146/annurev.biophys.050708.133724.

[48] Gal N, Lechtman-Goldstein D, Weihs D. Particle tracking in living cells: a review of the mean square displacement method and beyond. Rheol Acta 2013;52:425–43. https://doi.org/10.1007/s00397-013-0694-6.

[49] Hozé N, Holcman D. Statistical methods for large ensembles of superresolution stochastic single particle trajectories in cell biology. Annu Rev Stat Appl 2017;4:189–223. https://doi.org/10.1146/annurev-statistics-060116-054204.

[50] Höfling F, Franosch T. Anomalous transport in the crowded world of biological cells. Rep Prog Phys 2013;76:046602. https://doi.org/10.1088/0034-4885/76/4/046602.

[51] Manzo C, Garcia-Parajo MF. A review of progress in single particle tracking: from methods to biophysical insights. Rep Prog Phys 2015;78:124601. https://doi.org/10.1088/0034-4885/78/12/124601.

[52] Shen H, Tauzin LJ, Baiyasi R, Wang W, Moringo N, Shuang B, et al. Single particle tracking: from theory to biophysical applications. Chem Rev 2017;117:7331–76. https://doi.org/10.1021/acs.chemrev.6b00815.

[53] Zagato E, Forier K, Martens T, Neyts K, Demeester J, De Smedt S, et al. Single-particle tracking for studying nanomaterial dynamics: applications and fundamentals in drug delivery. Nanomedicine 2014;9:913–27. https://doi.org/10.2217/nnm.14.43.

[54] Kaerger J, Ruthven DM, Theodorou DN. Diffusion in Nanoporous Materials. Weinheim: Wiley-VCH Verlag; 2012.

[55] Kaerger J, Ruthven D. Diffusion in nanoporous materials: fundamental principles, insights and challenges. New J Chem 2016;40:4027–48. https://doi.org/10.1039/C5NJ0283.

[56] Crank J. The mathematics of diffusion. Oxford: Clarendon; 1970.

[57] Sobolev SL. Local non-equilibrium transport models. Physics-Uspekhi 1997;40(10):1043–53. https://doi.org/10.1070/PU1997v040n10ABEH000292.

[58] Sobolev SL, Dai W. Heat transport on ultrashort time and space scales in Nanosized systems: diffusive or wave-like? Materials 2022;15(12):4287. https://doi.org/10.3390/ma15124287.

[59] Joseph DD, Preciozi L. Heat wave. Rev Mod Phys 1989;61:41. https://doi.org/10.1103/RevModPhys.61.41.

[60] Novikov IA. Harmonic thermal waves in materials with thermal memory. J Appl Phys 1997;81:1067–72. https://doi.org/10.1063/1.363849.

[61] Galovic S, Kostoski D. Photothermal wave propagation in media with thermal memory. J Appl Phys 2003;93:3063–71. https://doi.org/10.1063/1.1540741.

[62] Cattaneo C. Sur une forme de l'equation de la chaleur eliminant le paradowe d'une propagation instantanee. C R Acad Sci 1958;247:431.

[63] Vernotte P. Sur quelques complications possible dans les phenomenes de conduction de la chaleur. C R Acad Sci 1961;252:2190.

[64] Jou D, Casas-Vazquez J, Lebon G. Extendid irreversible thermodynamics. Rep Prog Phys 1988;51:1105–79. https://doi.org/10.1088/0034-4885/51/8/002.

[65] Casas-V'azquez J, Jou D, Lebon G. Extended irreversible thermodynamics. Berlin: Springer; 1996.

[66] Fabrizio M, Franchi F. Delayed thermal models: stability and thermodynamics. Journal of Thermal Stresses 2014;37:160–73. https://doi.org/10.1080/01495739.2013.839619.

[67] Zimin BA, Sudenkov YuV. Analysis of the generalized heat equation for solution of the dynamic Thermoelasticity problem. Doklady Physics 2019;64(4):181–4. https://doi.org/10.1134/S1028335819040098.

[68] Ozisik MN, Tzou DY. On the wave theory of heat conduction. ASME J Heat Transfer 1994;116:526–35. https://doi.org/10.1115/1.2910903.

[69] Galovic S, Kostoski D, Suljovrujić E, Stamboliev G. Thermal wave propagation in media with thermal memory induced by pulsed laser irradiation. Rad Phys Chem 2003;67:459–61. https://doi.org/10.1016/S0969-806X(03)00085-9.

[70] Galovic S, Soskic Z, Popovic M, Cevizovic D, Stojanovic Z. Theory of photoacoustic effect in media with thermal memory. J Appl Phys 2014;116:02491. https://doi.org/10.1063/1.4885458.

[71] Lj K, Djordjevic SP, Milicevic E, Galovic SK, Suljovrujic D, Jacimovski M, et al. Photothermal response of polymeric materials including complex heat capacity. International Journal of Thermophysics 2022;43:68. https://doi.org/10.1007/s10765-022-02985-3.

[72] Kirsanov YuA, Kirsanov AYu, Yudakhin AE. Measurement of thermal relaxation and temperature damping time in a solid. High Temp 2017;55:114–9. https://doi.org/10.1134/S0018151X17010126.

[73] Ding Z, Chen K, Song B, et al. Observation of second sound in graphite over 200 K. Nat Commun 2022;13:285. https://doi.org/10.1038/s41467-021-27907-z.

[74] Huberman S, Duncan RA, Chen K, Song B, Chiloyan V, Ding Z, et al. Observation of second sound in graphite at temperatures above 100 K. Science 2019;364:375–9. https://doi.org/10.1126/science.aav3548.

[75] Polyanin AD, Vyazmin AV. Differential-difference heat-conduction and diffusion models and equations with a finite relaxation time. Theor Found Chem Eng 2013;47(3):217–24. https://doi.org/10.1134/S0040579513030081.

[76] Polyanin AD. Exact solutions to differential-difference heat and mass transfer equations with a finite relaxation time. Theor. Found. Chem. Eng. 2014;48(2):167–74. https://doi.org/10.1134/S0040579514020110.

[77] A. D. Polyanin, A. I. Zhurov, Exact solutions of linear and non-linear differential-difference heat and diffusion equations with finite relaxation time, International Journal of Non-Linear Mechanics, 54, 115–126, (2013). https://doi.org/https://doi.org/10.1016/j.ijnonlinmec.2013.03.011.

[78] Oldham KB, Spanier J. The fractional Calculus. New York: Academic; 1974.

[79] Podlubny I. Fractional differential equations. San Diego, CA: Academic Press; 1999.

[80] Tateishi A, Ribeiro HV, Lenzi EK. The role of the fractional time-derivative operators in anomalous diffusion. Front Phys 2017;5:1–5. https://doi.org/10.3389/fphy.2017.00052.

[81] Dzielinski A, Sierociuk D, Sarwas G. Some applications of fractional order calculus. BullPolish Acad Sci Tech Sci 2010;58:583–92. https://doi.org/10.2478/v10175-010-0059-6.

[82] Lenzi EK, Somer A, Zola RS, da Silva RS, Lenzi MK. A generalized diffusion equation: solutions and anomalous diffusion. Fluids 2023;8(34). https://doi.org/10.3390/fluids8020034.

[83] Caputo M, Fabrizio M. Admissible frequency domain response functions of dielectrics. Math Method Appl Sci 2014;38:930–6. https://doi.org/10.1002/mma.3118.

[84] Saxena RK, Saxena R, Kalla SL. Solution of space time fractional schroedinger equation occurring in quantum mechanics. Fract Calc Appl 2010;13:190–201. http://hdl.handle.net/10525/1648.

[85] Del Castillo Negrete D, Carreras BA, Lynch VE. Fractional diffusion in plasma turbulence. Phys of Plasmas 2004;11:3854–64. https://doi.org/10.1063/1.1767097.

[86] Magin R. Fractional Calculus in bioengineering. Redding: Begell House Publishers; 2006.

[87] Caputo M. Diffusion of fluids in porous media with memory. Geothermics 1999;28:113–30. https://doi.org/10.1016/S0375-6505(98)00047-9.

[88] Hilfer R. Experimental evidence for fractional time evaluation in glass forming materials. Chem Phys 2002;284:339–408. https://doi.org/10.1016/S0301-0104(02)00670-5.

[89] M. G. Trefry, D. S. Whyte, Analytical Solutions for Partitioned Diffusion in Laminates: I. Initial Value Problem with Steady Cauchy Conditions, Transport in Porous Media, 37 (1), 93–128, (1999). DOI:https://doi.org/10.1023/A:1006566125433.

[90] Carr EJ, March NG. Semi-analytical solution of multilayer diffusion problems with time-varying boundary conditions and general interface conditions. Applied Mathematics and Computation 2020;333:286–303.

[91] Kaoui B, Lacircella M, Pontrelli G. Mechanistic modeling of drug relese from multi-layer capsules, *Compt.* Biol. Med. 2018;93:149–57.

[92] Anissimov YG, Watkinson A. Modelling skin penetration using the Laplace transform technique. Skin Pharmacol Physiol 2013;26:286–94. https://doi.org/10.1159/000351924.

[93] Lian G, Chen L, Han L. An evaluation of mathematical models for predicting skin permeability. J Pharm Sci 2008;97(1):584–98. https://doi.org/10.1002/jps21074.

[94] Ellison CA, Tankerstey KO, Obringer CM, et al. Partition coefficient and diffusion coefficient determination of 50 compounds in human intact skin, isolated skin layer and isolated stratum corneum lipids. Toxicol In Vitro 2020;69, 104990. https://doi.org/10.1016/j.tiv.2020.104990.

[95] Li SK, Chautasart D. Skin permeation enhancement in aqueous solution: correction with equilibrium enhancer concentration and octanol/water partition coefficient. JPharm Sci 2019;108(1):350–77. https://doi.org/10.1016/s.xphs.2018.08.14.